AN INVESTIGATION ON THE EFFECT OF TENSILE LOADING ON THE DUCTILE TO BRITTLE TRANSITION TEMPERATURE OF FERRITIC STEEL

SB Bhimavarapu, AK Maheshwari, D Bhargava, BK Dutta* & SP Narayan
Advanced Materials & Processes Research Institute (CSIR), Bhopal, INDIA – 462064.
* Bhabha Atomic Research Center, Mumbai-400085, INDIA

ABSTRACT

Ferritic steel finds a high significance for nuclear applications due to its high strength and good ductility. The ductile to brittle transition (DBT) temperature for such material is determined by the Impact test. However, we have determined the DBT by the tensile loading at low strain rate. Our observation shows lower DBT temperature under tensile load. Since, the transition is a continuous and slow process; hence the failure probability is more perceptible when a component or a system is under tensile loading. The test method adopted could preciously determine the DBT temperature. The brittleness factors, determined by mechanical test are fully supported by the observed microstructure of the fractured samples. Weibull statistical analysis done from the 150 mechanical tests for failure probability is more precise than reported earlier.

INTRODUCTION

Ferritic steel, for its excellent mechanical properties like high strength and high ductility heed a significant space for versatile mechanical, domestic, structural and industrial applications. The venerable thermal properties enable this alloy to be economically rolled, extruded or forged into useful shapes. A good comparison with different mechanical behavior of this steel are mentioned elsewhere [1, 2]. In addition to the combination of these properties, the ability to sustain at low temperatures makes this alloy fit for fabricating the different components of water nuclear reactors. During the operation of the reactors, ferritic steels become brittle under the effect of irradiation. Such an irradiation embrittlement is manifested by an increase in the ductile-to-brittle transition temperature [3]. The reactor core re-flooding in the event of loss of coolant lowers the temperature of the core. As a result, the temperature of the material decreases and falls in the ductile–to-brittle domain. Cleavage fracture and ductile tearing are two competing mechanisms in the ductile-to-brittle transition regime of ferritic steels. In this regime, the steel structure can withstand significant amount of ductile tearing without substantial loss of its load bearing capacity. However, many experiments show that stable crack growth by ductile tearing eventually gives way to catastrophic cleavage fracture. The latter appears to be the critical failure mechanism limiting the load bearing capacity of the structure. Thus, it becomes important to estimate the cleavage failure probability of components operating at low temperatures or in irradiation environments (even if the temperature is in the ductile regime). An enhanced probabilistic model for cleavage fracture assessment of ferritic material has been discussed in [4]. Competing fracture mechanisms in the brittle-to-ductile transition region of ferritic steels can also be studied using theoretical decision models [5]. Such model depends on the relative energies of the different mechanisms.

Available information suggests that experimental data on cleavage fracture tend to be highly scattered. Two reasons have been offered for the large variations in measured cleavage fracture toughness at a given temperature within the transition region. First, cleavage fracture toughness in the transition region is controlled to a great extent by statistical sampling of a critical cleavage crack nucleus. Second, the level of stress triaxiality ahead of the crack tip is a strong function of the geometry of the crack and the amount of crack growth. Therefore the population of eligible particles for cleavage fracture depends implicitly on crack geometry and this population changes as the crack grows because of alterations in stress triaxiality. A detailed study regarding the Crack initiation in the brittle fracture w.r.t. ductile-brittle transition temperature for ferritic steels has been studied by Coates et al. [6].

Conventionally, the estimation of ductile to brittle transition temperature (DBT) is done by a series of impact tests such as Charpy and/or Izod. These impact tests are high strain rate tests, which do not suffice the usage of the material in practical applications. In view of the above there is a need for more tests for accessing the DBT regime of the material. Tensile test at slow strain rates is one of the solutions. Since the ductile and brittle fracture are two

different offsetting mechanisms that results under tensile loading and finally leads to cleavage fracture. **Garrison** made a precise study to present the mechanics and microstructural aspects of ductile fracture and to emphasize the interplay between the approaches [7]. The ductile fracture exhibits a substantial plastic deformation with high energy absorption before fracture, while the brittle fracture exhibits a little or no plastic deformation with low energy absorption before fracture. A physical model of fracture in materials describing a featured brittle crack imbedded in a plastically deformed medium is shown by R. Thomson [8].

EXPERIMENTAL SETUP AND TEST PROCEDURE

The tensile tests were conducted on ferritic steel (20MnMoNi5-5) specimens, supplied by BARC, Mumbai (Fig.1a & 1b). The basic test facility (Fig 2a) essentially comprised of a servo-hydraulic computer controlled Universal Testing Machine (BiSS, Bangalore make), cryostat capable of maintaining temperature up to -150^{o}C, cryo-can/ pressure vessel for holding & circulating liquid nitrogen, temperature controller cum indicator, specimen temperature indicator, nitrogen gas cylinder, laser extensometer, diametrical mechanical extensometer and so on. Typical photographic view of the test arrangement for testing ungrooved (conventional smooth tensile specimens) and grooved specimens are shown in (Figs. 2a. & 2b). For carrying out tests, the specimens were fixed in position with the help of holders and diametrical extensometer gripped over the specimen gauge diameter suitably. Laser Reflection tapes were fixed at the outer ends of the mechanical extensometer to serve as reference points for the laser extensometer to measure diametrical contraction. A chromel-alumel thermocouple (K-type) was placed in close contact with the specimen for measuring the specimen temperature during testing. Load was applied gradually until specimen fractured. The tensile tests were carried out at the cross head speeds of 0.03 and 0.3 mm per minute for grooved and ungrooved specimens with a gauge length of 2.5 and 25 mm respectively, to maintain a strain rate of $2x10^{-4}$ s^{-1}. The diametrical contraction was measured through the laser and diametrical (mechanical) extensometers and recorded along with corresponding load. The purpose of using both extensometers was to ensure the correctness of the measurement and to correct any discrepancy incurred in the recording due to ice deposition or drift of extensometer. This has helped in eliminating the repetition of any test due to the mal-functioning of the extensometers or fault in recording. The plots of load as a function of diametrical contraction for the grooved specimens were directly displayed on the monitor. In the case of un-grooved (smooth) specimens with uniform gauge diameter, axial extension was measured using the same laser extensometer only. Mechanical extensometer was not used because of high percentage of elongation (20-30%), beyond the range of extensometer. Displacement of the cross head (stroke), when normalized with respect to the corresponding gauge length of 25 mm for a typical (ungrooved) specimen, was also calculated to see the degree of correspondence of the laser extensometer measurement with that of the later.

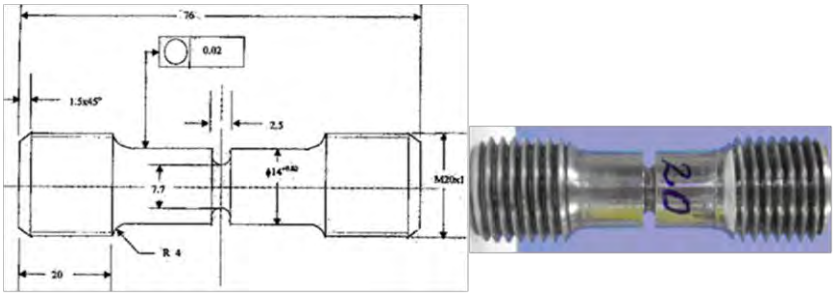

Fig 1a. Dimensional details of grooved tensile test specimen with actual photograph

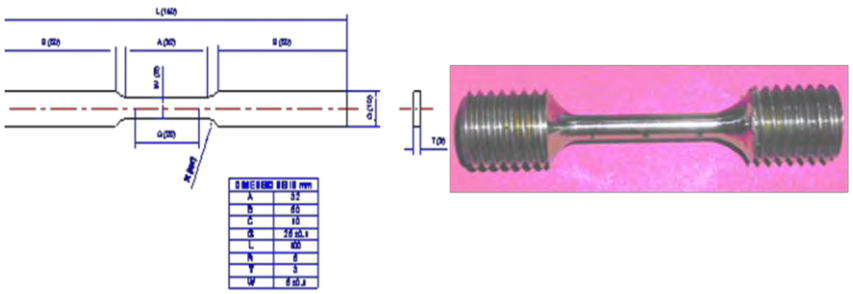

Fig 1b. Dimensional details of ungrooved tensile test specimen with actual photograph

Fig 2a. Basic test facility along with accessories (Exterior view)

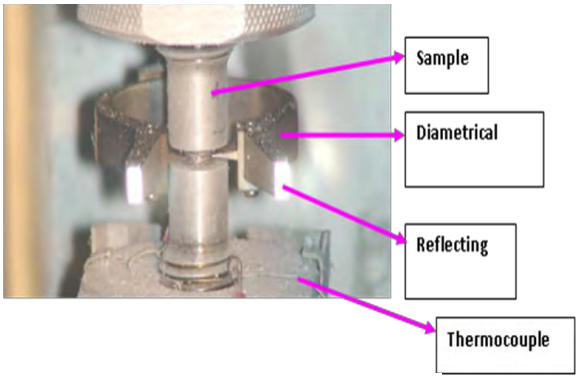

Fig 2b. Grooved specimen while testing at -100^{0}C (Interior view)

Subzero temperature was maintained in the cryo-chamber by passing liquid nitrogen vapour from the cryocan at positive atmospheric pressure. Pressurized nitrogen gas was passed through the cryocan at a controlled pressure and regulated flow rate for feeding the cryostat chamber with the required quantity of liquid nitrogen vapour. The controller in the cryo-chamber enabled to regulate the flow of the liquid nitrogen in the chamber to maintain the set temperature of the specimen within the accuracy of $\pm$1^{o}C. The laser extensometer placed outside the cryostat chamber was focused on the two ends of the mechanical extensometer containing the reflecting tape. A heating device (up to ~50^{o}C) was also placed near the window to remove fog/moisture deposition from outside on the window (Quartz glass) thereby enabling the laser extensometer to get the clearly reflected beam/signal back from the reference points (reflecting tapes) of the mechanical extensometer. Dimensions, like gauge diameter and length of the specimens, were measured prior to and after the tests. Diametrical contraction measured by the contact type (mechanical) and laser extensometers during the tensile tests has been recorded as a function of applied load.

A total of 150 grooved specimens at different subzero temperatures ranging from ambient to -150^{0}C and two specimens of uniform gauge length at each temperature were tested. 30 grooved specimens at each temperature were tested for Weibull statistics from which Beremin's local approach to estimate the brittle fracture.

RESULTS & DISCUSSION

Grooved Specimens

Tensile tests on grooved specimens have been carried out at five temperatures namely ambient, -10, -50, -100 and -150^{o}C for a set of 30 specimens at each temperature. Diametrical contraction with respect to the peak & breaking load of specimens recorded prior to failure at the test temperatures. Variation in the breaking load and diametrical contraction of the specimens at a typical temperature may be attributed to specimen-to-specimen dimensional variation initially, while variation in the corresponding load may be due to inhomogeneity in the material.

Comparisons of the load-diametrical contraction of the grooved specimens at different temperatures are shown in Fig.3a. This shows that with the decreasing test temperature, increasing trend in yield strength and tensile strength and a reducing trend in diametrical contraction prior to specimen failure. Fig 3b represents the stress-strain plot the grooved specimens tested at all temperatures.

Ungrooved Specimens

Tensile tests on smooth (ungrooved) specimens with uniform gauge diameter have been carried out at ambient, -10, -50, -100 and -150^{o}C. The axial extension values were measured directly with the laser extensometer. The machine compliance was determined at each test temperatures to compute the absolute axial extension of the specimens during testing. Grips were engaged against the threaded part of grooved specimen of 19 mm diameter and length 30mm, engaged with both the holders and then the load was applied. The machine compliance at an applied load of 60 kN was found to be a maximum of 0.80, 0.70, 0.69, 0.71 and 0.68 mm at ambient, -10, -50, -100 and -150^{0}C, respectively.

Observations made in this case were similar to those for the grooved tensile specimens. Load versus axial elongation plots for the specimens at the mentioned test temperatures after compliance correction are shown in Fig.3c. The axial extension shown in the figures and tables represents the absolute values. Fig.3d represents the stress-strain plots of the ungrooved specimens at all test temperatures. The yield strength increases with decreasing temperature improving the tensile strength. There is no noticeable change in the elongation of the specimens with respect to temperature. The yield load at ambient and 0^0C are nearly same, same for -50^0C and -100^0C and highest for -150^0C. All the specimens achieved nearly 0.3 strain as shown in Fig.3d.

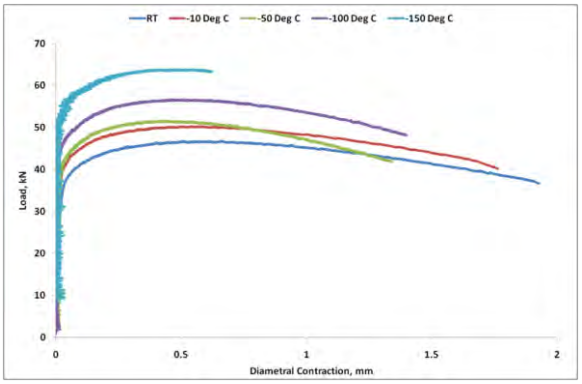

Fig3a. Load- diametral contraction curves of grooved specimens at ambient, -10,-50,-100 and -150^0C temperatures

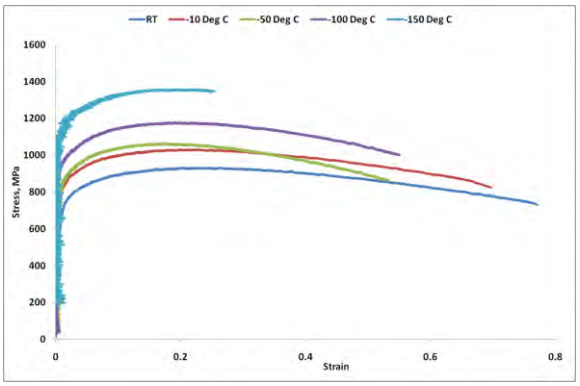

Fig 3b. Stress –Strain plots of grooved specimens ambient, -10,-50,-100 and -150^0C temperatures

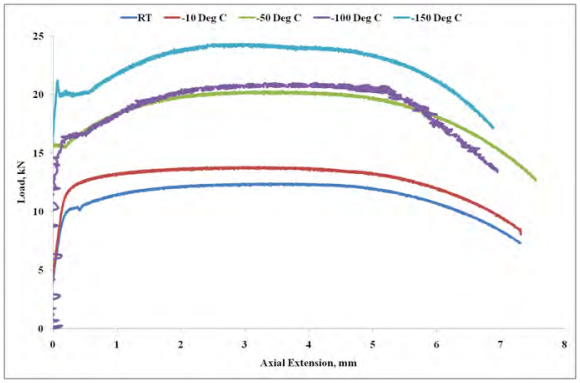

Fig. 3c. Load-Extension curves of ungrooved specimens at all test temperatures

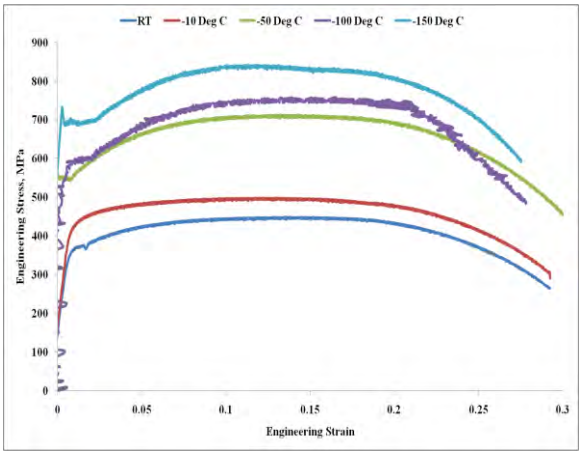

Fig. 3d. Stress-strain curves of ungrooved specimens at all test temperatures.

Tensile Properties

The relative brittleness is measured as the ratio between the breaking load to peak load. Brittleness (%) is decreased slightly at -10^{0}C than at the ambient temperature, but does not have phenomenal change upto -100^{0}C. But at -150^{0}C ~15% increase with a value of 97.8% was observed which is shown in Fig 4a., clearly shows that the material has a transition between -100^{0}C and -150^{0}C, which is drastically lower than that from the reported literature. This increase is mainly due to the slow strain rate testing of the specimens. Maximum load (P_m), Yield load (P_y) and Fracture load (P_f) increases with decrease in temperature as shown in Fig 4b. While in, % reduction in diameter, % reduction in area and nominal fracture strain decreases with decrease in temperature as shown in Fig. 4c. All these values are tabulated in Table.1.

Fractography

Fig. 5 (a & b) shows the fractographs of the specimens tested at -100^{0}C and -150^{0}C respectively. Fig 5a shows the cup cone fracture with nucleation point in its centre which clearly shows a ductile fracture also confirmed by the % brittleness as shown in Fig.4a. An ideal plastic material in which no strain hardening occurs would become unstable in tension and begin to neck just as soon as yielding took place. However, a real metal undergoes strain hardening, which tends to increase the load carrying capacity of the specimen as deformation increases. This effect is opposed by the gradual decrease in cross sectional area of the specimen as it elongates. Necking or localized deformation begins at maximum load, where there is increase in stress due to decrease in the cross sectional area of the specimen and becomes greater than the load carrying ability of the metal due strain hardening. When the maximum load is reached, the plastic deformation in a cylindrical tensile test piece becomes macroscopically heterogeneous and is concentrated in a small region. This phenomenon is called necking .The final fracture occurs in this necked region and has the characteristic appearance of a conical region on the periphery resulting from shear and a central flat region resulting from the voids created there. In materials where the second phase particles and inclusions are well bonded to the matrix, void nucleation is often the critical step, fracture occur soon after the voids form. When void nucleation occurs with little difficulty, the fracture properties are controlled by the growth and coalescence of voids, the growing voids reaches critical size, relative to their spacing and a local plastic instability develops between voids, resulting in failure.

Fig.5b. shows cleavage fracture which confirms the brittle fracture as shown in Fig.4a. Cleavage generally takes place by the separation of atomic bonds along well-defined crystal planes. Ideally, a cleavage fracture would have perfectly matching faces and be completely flat and featureless. However, structural materials are characteristically, polycrystalline with the grains more or less randomly oriented with respect to each other. Thus cleavage propagating through one grain will probably have to change direction as it crosses a grain or sub-grain boundary (sub-grains are regions within a grain that differ slightly in crystal orientation). Such changes in direction, results in the faceted fracture surface. In addition most structural material contain particles, precipitates or other imperfections that further complicate the fracture path, so that truly featureless cleavage is rare, even within a single grain or subgrain. The changes of orientation between grains and subgrains and the various imperfections produce markings on the fracture

surface that are characteristically associated with cleavage. The cleavage crack changes direction at the grain boundary in order to continue along the given crystallographic planes. The cleavage facets seen through the grains have a high reflectivity, which gives the fracture surface a shiny appearance. Sometimes the cleavage fracture surface shows some small irregularities-for example, the river markings. What happens is that, within a grain, cracks may grow simultaneously on two parallel crystallographic planes the two parallel cracks can then join together, by secondary cleavage or by shear, to form a step. Cleavage steps can be initiated by the passage of a screw dislocation. In general, the cleavage step will be parallel to the crack's direction of propagation and perpendicular to the plane containing the crack. As this configuration, would minimize the energy for the step formation by creating a minimum of additional surface. A large number of cleavage steps can join and form a multiple step. On the other hand, steps of opposite signs can join and disappearing. The junction of cleavage steps results in a figure of a river and its tributaries. River markings can appear by the passage of a grain boundary. When a crack passes through a grain boundary, it has to propagate in a grain with a different orientation [9]. Figure5b shows, the encounter of a cleavage crack with a grain boundary. After they meet, the crack should propagate on a cleavage plane that is oriented in a different manner. The crack can do this at various points and spread into the new grain. Such a process gives rise to the formation of a number of steps that can group together, generating a river marking. The convergence of tributaries is always in the direction of flow of the river. Cleavage is a common phenomenon observed in body centered cubic (BCC) and hexagonal close-packed (HCP) structures, particularly in iron and low-carbon steels (BCC). Tungsten, molybdenum, and chromium (all BCC) and zinc, beryllium, and magnesium (all HCP) are other examples of metals that commonly show cleavage.

Table.1: Tensile properties of Ferritic steel

Temp.	**Max. load Pm (kN)**	**Yield Load Py (kN)**	**Fracture load $P_{f\ (kN)}$**	**Tensile Strength $s_{b\ (GPa)}$**	**% Brittleness**	**Engineering Fracture Strength $s_{f\ (Gpa)}$**	**Reduction in diameter (%)**	**Reduction of Area Y%**	**Nominal Fracture Strain e_f**
-150^{0}C	64.5	53.64	61.21	232.8	97.8	220.93	12.46	23.38	0.1255
-100^{0}C	61.29	50.12	53.74	218.36	82.7	191.46	15.53	28.64	0.1553
-50^0 C	54.49	44.19	43.36	177.31	80.3	141.09	18.36	37.66	0.1845
-10^{0}C	50.39	38.62	40.69	150.26	79.2	121.36	22.35	39.68	0.2243
RT	44.59	35.59	37.54	133.05	80.4	109.32	23.23	41.06	0.2363

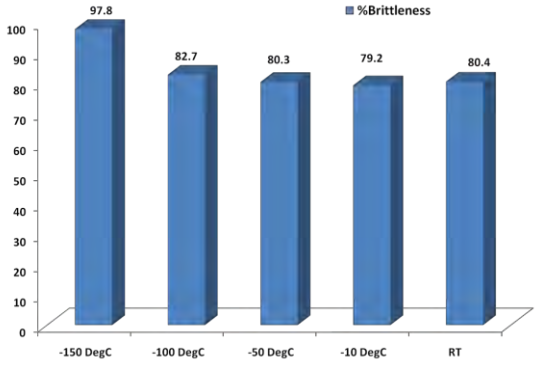

Fig.4a: Brittleness of Ferritc steel

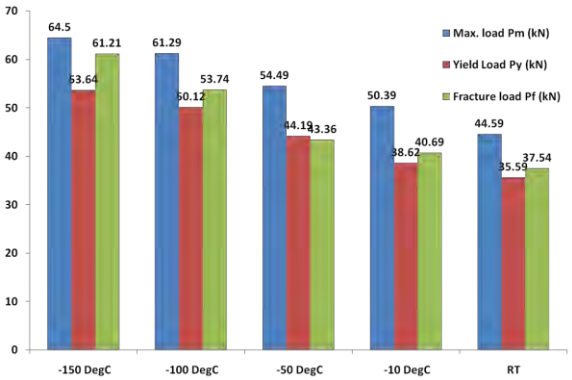

Fig 4b:

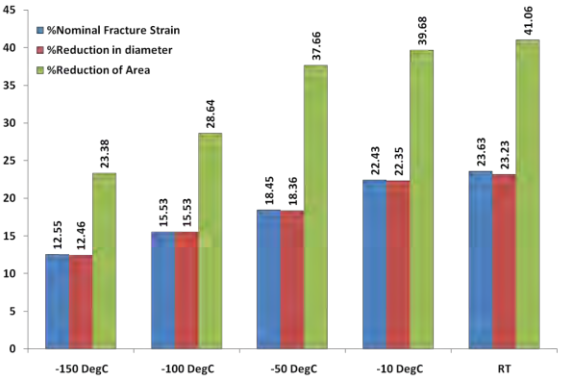

Fig 4c

Fig. 4.(b) & (c) Different tensile properties at different temperatures.

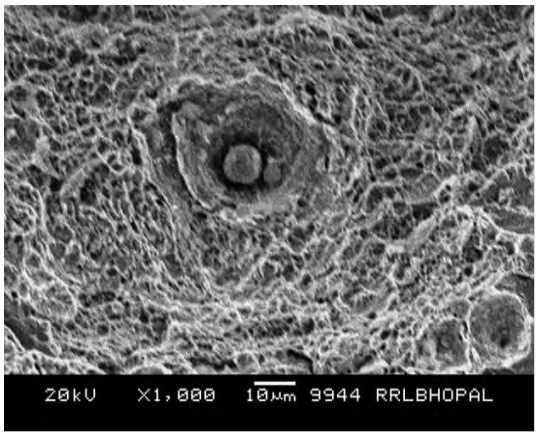

Fig.5a: Fractograph of ferric steel tested at -100^{0}C, showing cup & cone fracture, confirming the ductile fracture.

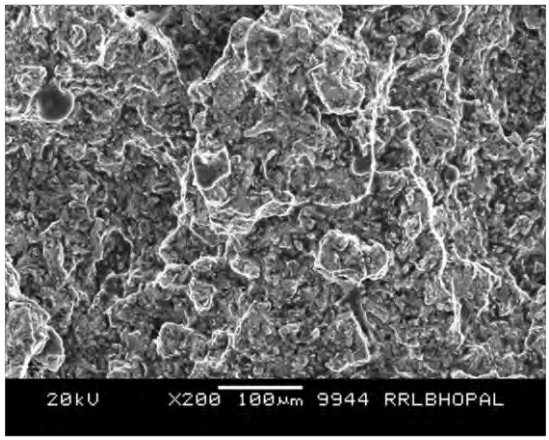

Fig.5b: Fractograph of ferric steel tested at -150^{0}C, showing cleavage fracture with river pattern, confirming the brittle fracture.

CONCLUSIONS

The use of laser extensometer has substantially improved the precision and reliability of the test. The conventional impact test method shows higher DBT temperature w.r.t. the tensile loading at low strain rate. Hence, the failure

probability significantly improves when a component or a system is under tensile loading. The method adopted could preciously determine the DBT temperature. Weibull statistics adds up more comprehensive information in determining the safety of nuclear components, under prolong uses. The determination of brittleness factor by mechanical test is fully supported by the observed microstructure of the fractured samples.

ACKNOWLEDGEMENT

The authors from AMPRI are grateful to the Director for the permission given to publish this paper. The project has been sponsored by BARC, Mumbai and funded by BRNS (Project no. 2004/36/34-BRNS/2305- 2005)

REFERENCES

1. A. Rusinek, J.A. Rodríguez-Martínez, J.R. Klepaczko, R.B. Pe˛cherski, "Analysis of thermo-visco-plastic behaviour of six high strength steels", Materials and Design. Vol. 30, 2009, pp. 1748–1761.
2. S. Cicero, F. Gutierrez-Solana , A.J. Horn, "Experimental analysis of differences in mechanical behaviour of cracked and notched specimens in a ferritic–pearlitic steel: Considerations about the notch effect on structural integrity", Engineering Failure Analysis. Vol. 16(7), 2009, pp. 2450-2466.
3. J.F. Knott, C.A. English, D.R. Weaver, D.P.G. Lidbury, "Views of TAGSI on the effects of gamma irradiation on the mechanical properties of irradiated ferritic steel reactor pressure vessels", International Journal of Pressure Vessels and Piping. Vol. 82, 2005, pp. 929–940.
4. Jörg Hohe, Volker Hardenacke, Sabrina Luckow, Dieter Siegele, "An enhanced probabilistic model for cleavage fracture assessment accounting for local constraint effects". Engineering Fracture Mechanics. Vol 77(18), 2010, Pp.3573-3591
5. G. E. Smith, A. G. Crocker, R. Moskovic and P. E. J. Flewitt, "Competing fracture mechanisms in the brittle-to-ductile transition region of ferritic steels", Materials Science and Engineering A. Vol. 387, 2004, pp. 367-371.
6. M. Coates, A. Kumar and S. G. Roberts, "Crack initiation in the brittle fracture of ferritic steels", Blackwell Publishing Ltd. Fatigue Fract Engng Mater Struct. 29, 661–671.
7. W.M. Garrison Jr, N.R. Moody, "Ductile fracture", Journal of Physics and Chemistry of Solids. Vol. 48 (11), 1987, pp. 1035-1074.
8. R. Thomson, "Brittle fracture in a ductile material with application to hydrogen embrittlement", Journal of Materials Science. Vol. 13, 1978, pp. 128-142.
9. Ján Bo anský, Tibor mida,"Deformation twins -probable inherent nuclei of cleavage fracture in ferritic steels", Materials Science and Engineering A. Vol. 323 (1-2) 2002, 198-205.